A novel interaction between FlnA and Syk regulates platelet ITAM-mediated receptor signaling and function

Hervé Falet,[1,4] Alice Y. Pollitt,[6] Antonija Jurak Begonja,[1,4] Sarah E. Weber,[1,4] Daniel Duerschmied,[2,3,5] Denisa D. Wagner,[2,3,5] Steve P. Watson,[6] and John H. Hartwig[1,4]

[1]Division of Translational Medicine, Brigham and Women's Hospital, [2]Immune Disease Institute, [3]Program in Cellular and Molecular Medicine, Children's Hospital Boston, and [4]Department of Medicine and [5]Department of Pathology, Harvard Medical School, Boston, MA 02115
[6]Centre for Cardiovascular Sciences, Institute for Biomedical Research, College of Medical and Dental Sciences, University of Birmingham, Birmingham B15 2TT, England, UK

Filamin A (FlnA) cross-links actin filaments and connects the Von Willebrand factor receptor GPIb-IX-V to the underlying cytoskeleton in platelets. Because FlnA deficiency is embryonic lethal, mice lacking FlnA in platelets were generated by breeding $FlnA^{loxP/loxP}$ females with GATA1-Cre males. $FlnA^{loxP/y}$ GATA1-Cre males have a macrothrombocytopenia and increased tail bleeding times. FlnA-null platelets have decreased expression and altered surface distribution of GPIbα because they lack the normal cytoskeletal linkage of GPIbα to underlying actin filaments. This results in ∼70% less platelet coverage on collagen-coated surfaces at shear rates of 1,500/s, compared with wild-type platelets. Unexpectedly, however, immunoreceptor tyrosine-based activation motif (ITAM)- and ITAM-like–mediated signals are severely compromised in FlnA-null platelets. FlnA-null platelets fail to spread and have decreased α-granule secretion, integrin αIIbβ3 activation, and protein tyrosine phosphorylation, particularly that of the protein tyrosine kinase Syk and phospholipase C–γ2, in response to stimulation through the collagen receptor GPVI and the C-type lectin-like receptor 2. This signaling defect was traced to the loss of a novel FlnA–Syk interaction, as Syk binds to FlnA at immunoglobulin-like repeat 5. Our findings reveal that the interaction between FlnA and Syk regulates ITAM- and ITAM-like–containing receptor signaling and platelet function.

CORRESPONDENCE
Hervé Falet:
hfalet@rics.bwh.harvard.edu.

Abbreviations used: CHO, Chinese hamster ovary; CLEC-2, C-type lectin-like receptor 2; CRP, collagen-related peptide; FlnA, filamin A; GPCR, G protein–coupled receptor; ITAM, immunoreceptor tyrosine-based activation motif; PLC-γ2, phospholipase C-γ2; PRP, platelet-rich plasma; VWF, Von Willebrand factor.

The filamin family consists of three large dimeric proteins (filamin A [FlnA], FlnB, and FlnC) that cross-link actin filaments, tether membrane glycoproteins, and serve as scaffolds for signaling intermediates (Stossel et al., 2001; Zhou et al., 2010). The most abundant isoform of the family, FlnA, is encoded by the X chromosome in humans and mice (Feng and Walsh, 2004; Robertson, 2005). FlnA is composed of an N-terminal actin-binding domain followed by 24 Ig repeats, the C-terminal of which mediates their dimerization (Pudas et al., 2005). Human melanoma cells that lack FlnA have poor motility and continuous membrane blebbing (Cunningham et al., 1992; Flanagan et al., 2001). *FLNA* mutations have been associated with periventricular heterotopia, Ehlers-Danlos Syndrome, or familial cardiac valvular dystrophy (Fox et al., 1998; Robertson et al., 2003; Sheen et al., 2005; Kyndt et al., 2007; Unger et al., 2007). Loss of FlnA in mice results in embryonic lethality caused by pericardiac and visceral hemorrhage, severe cardiac structural defects, and aberrant vascular patterning (Feng et al., 2006; Hart et al., 2006).

Platelets predominantly express FlnA (5 μM), although a small amount of FlnB is also expressed (<0.5 μM). Platelet FlnA has a critical structural role in attaching the Von Willebrand Factor (VWF) receptor complex GPIb-IX-V to the underlying actin cytoskeleton. aa 556–577 in

The Rockefeller University Press $30.00
J. Exp. Med. Vol. 207 No. 9 1967-1979
www.jem.org/cgi/doi/10.1084/jem.20100222

The Journal of Experimental Medicine

the cytoplasmic tail of GPIbα constitutively interacts with FlnA Ig repeat 17 (Nakamura et al., 2006), and the loss of GPIbα in mice results in enlarged platelets, a phenotype which can be rescued by expression of a chimeric protein construct containing the cytoplasmic domain of human GPIbα (Ware et al., 2000; Kanaji et al., 2002). FlnA binding facilitates GPIbα surface expression in Chinese hamster ovary (CHO) cells (Feng et al., 2005), and the interaction between FlnA and GPIbα has been reported to influence VWF receptor function, although conflicting effects are found in the literature. CHO cells transfected with GPIbα mutants that lack the FlnA binding site have decreased VWF binding (Dong et al., 1997; Schade et al., 2003), VWF-induced cell aggregation (Mistry et al., 2000), and/or adhesion to a VWF matrix under high shear (Cranmer et al., 1999; Williamson et al., 2002; Cranmer et al., 2005). In contrast, another study has shown that FlnA binding to GPIbα negatively regulates VWF binding to CHO cells and CHO cell adhesion under both static and flow conditions (Englund et al., 2001). Platelets treated with cell-permeable peptide mimics of the FlnA binding site on GPIbα have decreased ability to activate their fibrinogen receptor, the integrin αIIbβ3, and change shape in response to VWF stimulation, suggesting that the interaction between FlnA and GPIbα positively modulates signaling events initiated by VWF in platelets (Feng et al., 2003; David et al., 2006).

In this study the role of FlnA was probed in platelets. Mouse platelets lacking FlnA were generated by breeding $FlnA^{loxP/loxP}$ females with GATA1-Cre males (Jasinski et al., 2001). Offspring $FlnA^{loxP/y}$ GATA1-Cre males have <15% of normal blood platelet count, and their platelets lack FlnA. As expected, FlnA-null platelets are large, lack normal actin-GPIbα membrane attachments, and have an altered distribution of GPIbα on their surface. However, FlnA-null platelets surprisingly also have severe functional impairment in signaling responses downstream of the immunoreceptor tyrosine-based activation motif (ITAM)– and ITAM-like–mediated signal receptors GPVI and C-type lectin-like receptor 2 (CLEC-2). This specific signaling defect results from the loss of a novel and direct FlnA–Syk interaction mediated through Ig repeat 5 of FlnA. As a consequence, Syk is mistargeted in FlnA-null platelets, and ITAM signaling that normally leads to actin assembly, α-granule secretion, integrin αIIbβ3 activation, and protein tyrosine phosphorylation is interrupted. FlnA is, therefore, required for normal ITAM- and ITAM-like–based signaling responses.

RESULTS

Mild thrombocytopenia in female mice carriers for FlnA deficiency

FlnA deficiency in mice results in lethality in utero as a result of pericardiac and visceral hemorrhage, severe cardiac structural

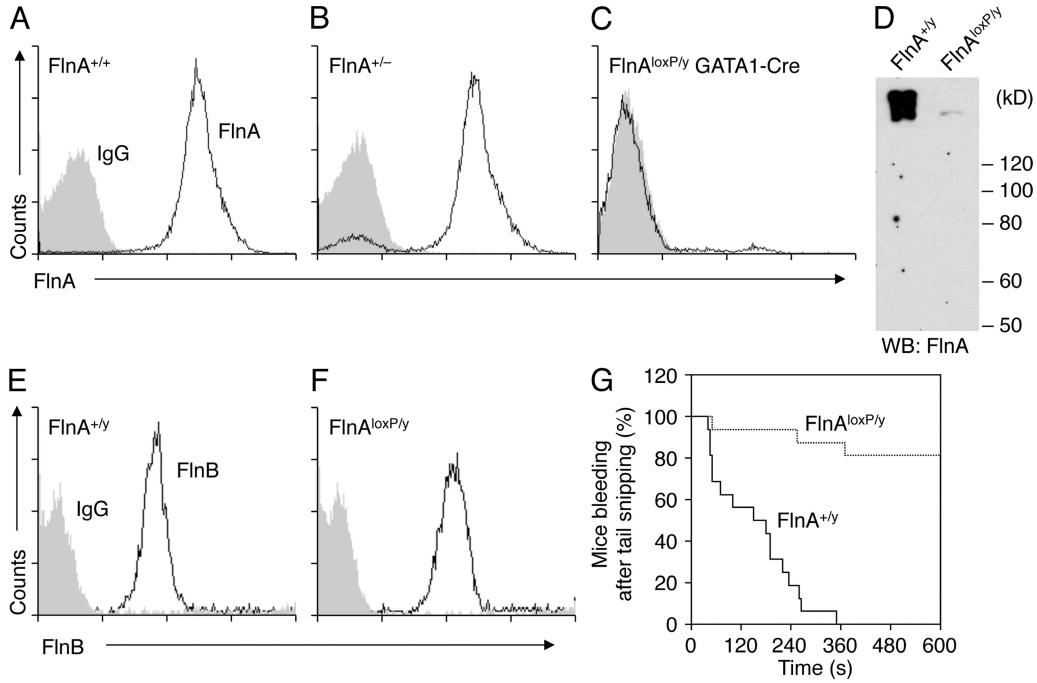

Figure 1. FlnA/B expression in platelets and mouse tail bleeding time. (A–C) FlnA expression in $FlnA^{+/+}$ (A), $FlnA^{+/-}$ (B), and $FlnA^{loxP/y}$ GATA1-Cre (C) platelets was evaluated by intracellular flow cytometry using a rabbit antibody directed against mouse FlnA (thin line). A nonspecific rabbit antibody was used as a control (gray area). (D) Lysates corresponding to 5×10^6 $FlnA^{+/y}$ GATA1-Cre and $FlnA^{loxP/y}$ GATA1-Cre platelets were subjected to SDS-PAGE and probed with anti-FlnA antibody, as indicated. FlnB expression in $FlnA^{+/y}$ GATA1-Cre (E) and $FlnA^{loxP/y}$ GATA1-Cre (F) platelets was evaluated by intracellular flow cytometry using a rabbit antibody directed against human FlnB (thin line). A nonspecific rabbit antibody was used as a control (gray area). Results are representative of five independent experiments. (G) $FlnA^{+/y}$ GATA1-Cre ($n = 16$) and $FlnA^{loxP/y}$ GATA1-Cre ($n = 16$) mouse tail bleeding times were statistically analyzed by the Kaplan-Meier method. $FlnA^{+/y}$ GATA1-Cre mice show a median bleeding time of 165 s. $FlnA^{loxP/y}$ GATA1-Cre mice displayed a severe bleeding phenotype, with 13 of 16 (81%) mice having bleeding times that exceeded 600 s (log-rank $p = 1.27 \times 10^{-7}$).

Table I. Complete blood count in 6–8-wk-old $FlnA^{+/+}$ and $FlnA^{+/-}$ female mice

Parameter	$FlnA^{+/+}$ (n = 17)	$FlnA^{+/-}$ (n = 14)	P-value
Erythrocytes	8,934 ± 2297	8,923 ± 2565	NS
Lymphocytes	4.46 ± 1.43	6.28 ± 2.16	<0.01
Granulocytes	0.30 ± 0.11	0.50 ± 0.24	<0.01
Platelets	994 ± 294	678 ± 278	<0.01
Mean platelet volume (fl)	6.3 ± 0.2	6.8 ± 0.9	<0.05

Results are expressed as mean × 10^3 cells/µl ± SD. NS indicates not significant.

defects, and aberrant vascular patterning (Feng et al., 2006; Hart et al., 2006). Because the *FLNA* gene is located on the X chromosome, we determined whether it conferred survival value to platelets in 6–8-wk-old heterozygous female mice carrying both one WT and one deleted *FLNA* gene. $FlnA^{+/-}$ females had a mild thrombocytopenia (Table I). Their blood platelet count was 678 ± 278 × 10^3/µl (mean ± SD; n = 14), compared with 994 ± 294 × 10^3/µl (n = 17; $P < 0.01$) in WT female littermates, revealing a reduction of 32%. The mean platelet volume was increased by 8%, compared with WT female littermates ($P < 0.05$). $FlnA^{+/-}$ females also had increased leukocyte count, notably lymphocytes and granulocytes. Erythrocyte counts were normal.

Platelets were isolated from $FlnA^{+/-}$ and WT mouse blood, fixed and permeabilized, and FlnA expression was determined by intracellular flow cytometry using a rabbit antibody directed against FlnA hinge 1 (Fig. 1, A and B). Two populations, one positive and one negative, were identified in $FlnA^{+/-}$ females, compared with only one single FlnA-positive population in WT female littermates. 95 ± 2% (mean ± SD; n = 14) of platelets isolated from $FlnA^{+/-}$ females contained FlnA, which was significantly greater than the expected 50% ($P < 0.0001$). FlnA-null platelets were large, as indicated by forward and side scatter dot plot analysis (unpublished data).

Generation of mice carrying platelets that selectively lack FlnA

GATA1-Cre transgenic mice were used to excise the $FlnA^{loxP}$ gene in the erythroid/megakaryocytic lineage (Jasinski et al., 2001). $FlnA^{loxP/loxP}$ females were bred with GATA1-Cre males. In this cross, all offspring expressed GATA1-Cre, and females were heterozygous and males hemizygous for $FlnA^{loxP}$. Only 79 (14.2%) out of the 555 offspring obtained were males. Analysis of embryos collected at different stages of development showed a high embryonic mortality associated with complex developmental abnormalities (unpublished data), which is consistent with leaky GATA1-Cre expression in early embryogenesis leading to $FlnA^{loxP}$ gene recombination in multiple nonhematopoietic tissues (Mao et al., 1999; Jasinski et al., 2001).

Macrothrombocytopenia in male mice with platelets lacking FlnA

Blood counts revealed a macrothrombocytopenia in 6–8-wk-old $FlnA^{loxP/y}$ GATA1-Cre males (Table II). The mean blood platelet count was 284 ± 70 × 10^3/µl (n = 16), compared with 1,773 ± 403 × 10^3/µl (n = 19; $P < 0.001$) in control $FlnA^{+/y}$ GATA1-Cre males, an 84% reduction. The mean volume of FlnA-null platelets was 13.2 ± 2.1 fl, compared with 6.3 ± 0.5 fl in control males ($P < 0.001$). $FlnA^{loxP/y}$ GATA1-Cre males had increased lymphocyte count compared with $FlnA^{+/y}$ GATA1-Cre males. Other blood cell parameters were in the normal range. The ∼2.1-fold increased platelet volume correlated with a ∼2.7-fold increase in total protein content, from 927 ± 95 fg per FlnA-expressing platelet (n = 6) to 2,464 ± 263 fg per FlnA-null platelet (n = 9; $P < 0.0001$), as determined by Bradford assay using BSA as standard.

FlnA expression was evaluated in platelets isolated from $FlnA^{+/y}$ GATA1-Cre and $FlnA^{loxP/y}$ GATA1-Cre males by intracellular flow cytometry (Fig. 1 C) and by SDS-PAGE and immunoblotting (Fig. 1 D). FlnA expression was absent in most platelets isolated from $FlnA^{loxP/y}$ GATA1-Cre males. A small population (<5%) of FlnA-containing platelets could be detected in some animals, suggesting mosaic GATA1-Cre expression, rendering incomplete $FlnA^{loxP}$ excision. In contrast, FlnB expression levels appeared to be increased by approximately twofold in FlnA-null platelets, compared with WT (Fig. 1, E and F).

Table II. Complete blood count in 6–8-wk-old $FlnA^{+/y}$ GATA1-Cre and $FlnA^{loxP/y}$ GATA1-Cre male mice

Parameter	$FlnA^{+/y}$ (n = 19)	$FlnA^{loxP/y}$ (n = 16)	P-value
Erythrocytes	8,648 ± 1596	8,753 ± 2234	NS
Lymphocytes	4.55 ± 2.17	7.71 ± 2.26	<0.05
Granulocytes	0.93 ± 0.66	0.74 ± 0.34	NS
Platelets	1773 ± 403	284 ± 70	<0.001
Mean platelet volume (fl)	6.3 ± 0.5	13.2 ± 2.1	<0.001

Results are expressed as mean × 10^3 cells/µl ± SD. NS indicates not significant.

Increased tail bleeding time in mice with platelets lacking FlnA

FlnA$^{loxP/y}$ GATA1-Cre males had prolonged tail bleeding times (Fig. 1 G). 13 (81%) out of 16 FlnA$^{loxP/y}$ GATA1-Cre males had tail bleeding >10 min, which was our selected end measurement point. In contrast, the median tail bleeding time for FlnA$^{+/y}$ GATA1-Cre males was 165 s (n = 16; log-rank P = 1.27×10^{-7}).

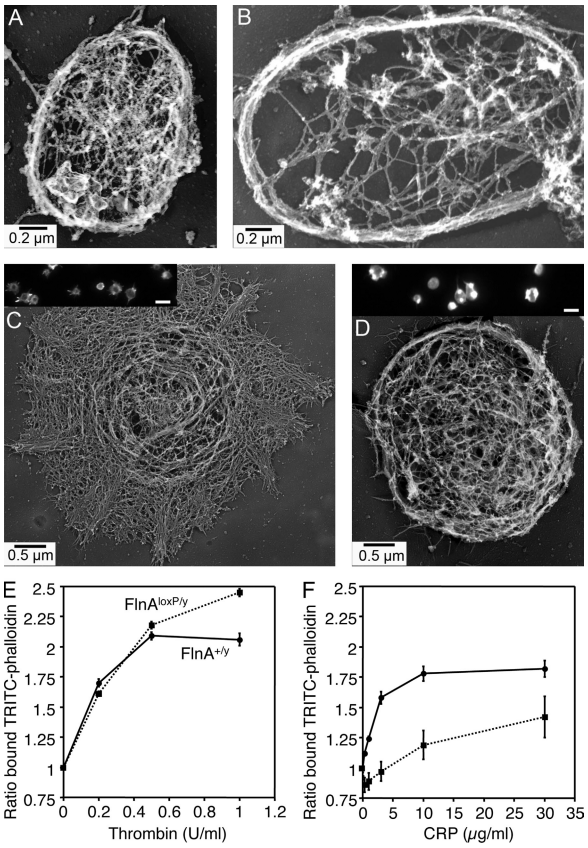

Figure 2. Role of FlnA expression in platelet morphology. (A and B) Representative cytoskeleton from a control FlnA$^{+/y}$ GATA1-Cre (A) or a FlnA$^{loxP/y}$ GATA1-Cre (B) resting platelet. Resting platelet cytoskeletons were prepared for the electron microscope by attachment to polylysine-coated coverslips in a permeabilizing PHEM buffer containing 0.75% Triton X-100, followed by fixation with 1% glutaraldehyde, and freezing in water, freeze drying, and metal casting. The FlnA-null cytoskeleton is enlarged and has a marginal microtubule ring, but the bulk of the cytoplasmic F-actin dissociates because of insufficient cross-linking of the actin filaments in the absence of FlnA. Bars, 0.2 µm. (C and D) Structure of the active cytoskeleton. FlnA$^{+/y}$ GATA1-Cre platelets (C) or FlnA$^{loxP/y}$ GATA1-Cre (D) were adhered to CRP-coated coverslips by centrifugation and incubated for 10 min at 37°C. Cells were then permeabilized in Triton X-100 in PHEM buffer containing 0.01% glutaraldehyde and processed for the electron microscopy as described. Bars, 0.5 µm. (Insets) Platelets were attached to and incubated on CRP-coated coverslips as in C and D and fixed with 3.7% formaldehyde in PBS for 30 min. F-actin was stained using 0.1% Triton X-100 in PBS and 0.1 µm Alexa Fluor 568 phalloidin. Bars, 5 µm. (E and F) Actin assembly. FlnA$^{+/y}$ GATA1-Cre and FlnA$^{loxP/y}$ GATA1-Cre platelets were activated with various concentrations of thrombin (E) or CRP (F) for 2 min at 37°C, as indicated. Platelets were fixed and permeabilized, washed, incubated with TRITC-labeled phalloidin, and analyzed by flow cytometry. Results are the ratio between the mean fluorescence of activated versus resting platelets and represent the mean ± SE of four independent experiments.

Structure of platelets lacking FlnA

Loss of the GPIbα–FlnA interaction alters the morphology of the resting platelet and its underlying cytoskeleton. Platelets isolated from FlnA$^{loxp/y}$ GATA1-Cre male mice are large but discoid, ∼4.0 µm in diameter at their longest axis, compared with ∼2.5 µm in controls. Fig. 2 (A and B) shows representative electron micrographs of the cytoskeletons of FlnA-null platelets prepared by removing the plasma membrane in the absence of glutaraldehyde with Triton X-100 detergent. In the absence of fixative, the bulk of the filaments composing the cytoskeleton are lost. In other words, cytoskeletal integrity is diminished as the bulk of the F-actin, but not the microtubule ring, rapidly dissociates from the cytoskeleton when FlnA-null platelets are permeabilized in buffers that normally stabilize an intact F-actin cytoskeleton. The percentage of

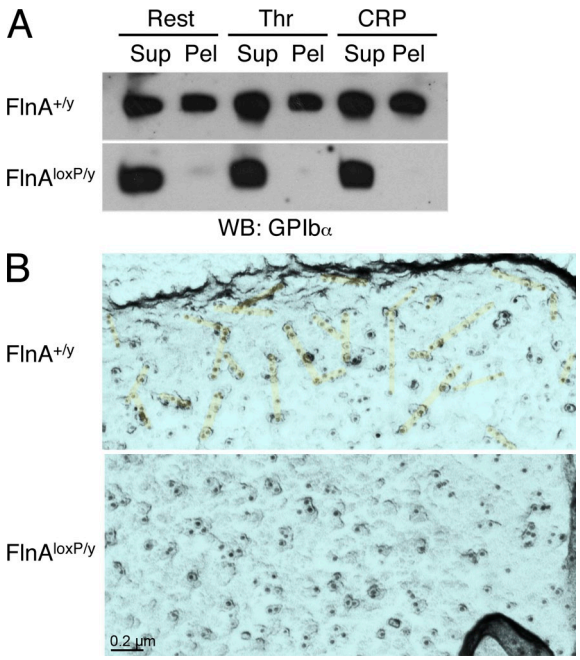

Figure 3. VWF receptor distribution in FlnA–null platelets. (A) GPIbα is not linked to the cytoskeleton of FlnA-null platelets. FlnA$^{+/y}$ GATA1-Cre and FlnA$^{loxP/y}$ GATA1-Cre platelets were activated or not (Rest) with 0.5 U/ml thrombin (Thr) or 3 µg/ml CRP for 5 min, as indicated. Triton X-100 soluble (Sup) and insoluble (Pel) fractions were collected by centrifugation of platelet lysates at 100,000 *g* for 30 min at 4°C, subjected to SDS-PAGE, and probed with a rat anti-GPIbα antibody. Results are representative of three independent experiments. (B) Distribution of anti-GPIbα gold on the surface of FlnA$^{+/y}$ GATA1-Cre and FlnA$^{loxP/y}$ GATA1-Cre platelets. GPIbα is found in linear arrays on the WT platelet surface. Arrays are highlighted with yellow shading. Particle counts revealed that 74.9 ± 5.9% of the total surface gold are in linear arrays composed of three or more particles. Only 13.1 ± 6.0% of the gold was arrayed on the FlnA-null platelet surface. Results are representative of five independent platelets for each mouse (0.5-µm^2 area on each).

Table III. Expression of major surface glycoproteins on FlnA-null platelets

Platelet glycoprotein	FlnA$^{+/y}$	FlnA$^{loxP/y}$	P-value
GPIbα (CD42b)	62.6 ± 3.2	34.2 ± 3.7	<0.005
GPIbβ (CD42c)	330.7 ± 43.2	251.1 ± 5.9	<0.05
GPIX (CD42a)	37.0 ± 6.3	27.8 ± 1.9	NS
GPV (CD42d)	67.3 ± 10.7	46.8 ± 4.1	NS
GPIIIa (CD61, integrin β3)	45.9 ± 17.1	152.4 ± 16.5	<0.005
GPVI	12.8 ± 2.8	17.9 ± 1.4	<0.05

The binding of fluorescently labeled antibodies directed against the platelet glycoproteins indicated above was measured by flow cytometry. Data are expressed as mean fluorescence intensity bound to the surface of FlnA$^{+/y}$ GATA1-Cre and FlnA$^{loxP/y}$ GATA1-Cre platelets and represent mean ± SD (n = 4–5 for each independent group). NS indicates not significant.

actin assembled into filaments was, however, comparable in the FlnA-null and WT platelets, representing 40% of the total actin levels. Because FlnA-null platelets are larger, they contain more total actin filaments than the control cells.

FlnA-null platelets adhere to the collagen-related peptide (CRP)–coated surfaces, which are specific for the collagen receptor GPVI but spread poorly, and have one or more unusual F-actin enriched foci within their cytoplasm (Fig. 2, C and D). In the electron microscope, these foci are aggregates of membrane skeleton and F-actin. In contrast, WT platelets activate on CRP-coated surfaces, spread, and generate blunt filopodia that are enriched in newly assembled F-actin, as indicated by both Alexa-phalloidin staining of F-actin and electron microscopy.

Fig. 2 (E and F) also shows that the limited shape change reaction of FlnA-null platelets to CRP results from a blunted actin assembly process. Although the F-actin assembly response mediated by the G protein–coupled receptor (GPCR) agonist thrombin is normal, FlnA-null platelets mount only a modest shape change and actin assembly reaction after CRP ligation of GPVI.

GPIbα expression and distribution in FlnA-null platelets

Expression of major platelet surface glycoproteins on FlnA-null platelets was examined by flow cytometry (Table III). FlnA deficiency resulted in a diminution of the expression of the VWF receptor, the GPIb-IX-V complex. Expression of the GPIbα (CD42b) subunit was reduced by 45% and that of GPIbβ (CD42c), GPV (CD42d), and GPIX (CD42a) by 25–30%. In contrast, expression of the fibrinogen receptor subunit, the integrin β3 (GPIIIa and CD41), and the collagen receptor GPVI was increased by 230 and 40%, respectively.

To demonstrate that the loss of FlnA results in untethered VWF complexes, the attachment of GPIbα to the actin cytoskeleton of FlnA-null platelets was evaluated (Fig. 3 A). FlnA$^{+/y}$ GATA1-Cre and FlnA$^{loxP/y}$ GATA1-Cre platelets were lysed in PHEM buffer containing Triton X-100, and F-actin was collected by centrifugation at 100,000 *g* for 30 min (Falet et al., 2002). We found that 41 ± 4% of total GPIbα was recovered in the Triton X-100–insoluble fraction of resting FlnA-positive platelets, which is consistent with earlier

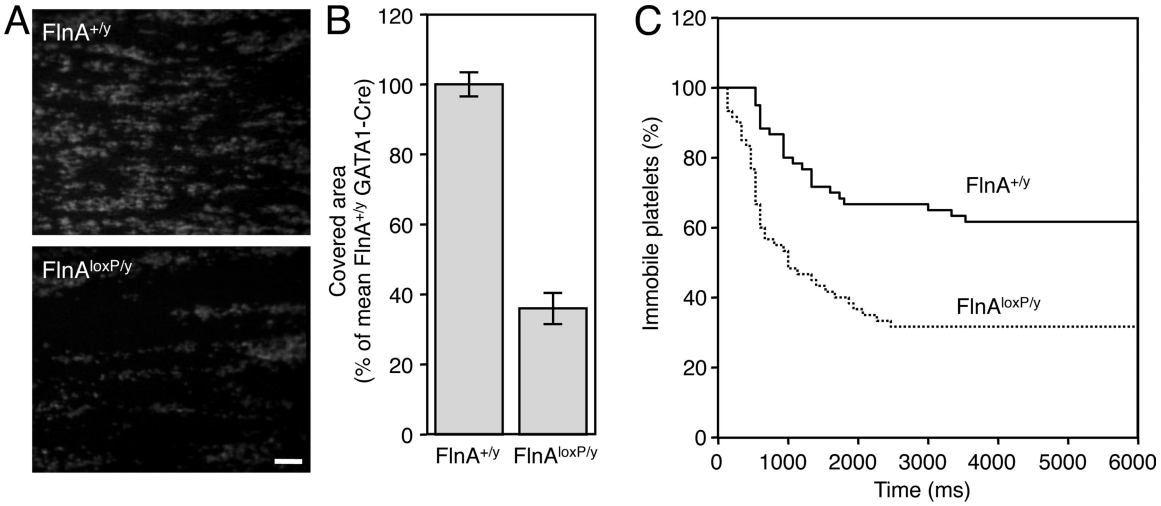

Figure 4. Platelet adhesion to collagen-bound VWF under arterial shear conditions. (A) After 3 min of perfusion of identical concentrations of labeled platelets in whole blood over collagen-coated surfaces at 1,500/s, ∼20% of the surface was covered by FlnA$^{+/y}$ GATA1-Cre platelets. Bar, 50 µm. (B) Mean of FlnA$^{+/y}$ GATA1-Cre platelets was set to 100% for better comparability. FlnA$^{loxP/y}$ GATA1-Cre platelet fluorescence covered 70% less area than FlnA$^{+/y}$ GATA1-Cre platelets. Error bars represent mean ± SEM (n = 6 mice). (C) Dwell time of 60 individual platelets per group under the same experimental conditions was significantly shorter in FlnA$^{loxP/y}$ than in FlnA$^{+/y}$ GATA1-Cre platelets. One-fifth of FlnA-null platelets detached after <500 ms under arterial shear conditions, whereas all FlnA$^{+/y}$ GATA1-Cre platelets dwelled for >500 ms. Results are representative of three independent experiments.

accounts of ~50% of GPIbα associated with the resting cytoskeleton (Fox, 1985a,b). In contrast, all GPIbα remained Triton X-100 soluble in FlnA$^{loxP/y}$ GATA1-Cre platelets. The lack of a cytoskeletal linkage altered the VWF receptor topology such that it was dispersed randomly across the platelet surface (Fig. 3 B). Particle counts revealed that only 10.6 ± 3.4% of GPIbα was arrayed into linear rows in FlnA-null platelets, compared with 72.0 ± 6.2% in WT controls (5 μm^2 area; $n = 5$), as described previously (Hoffmeister et al., 2003).

Platelet adhesion under arterial shear condition

The functionality of FlnA$^{loxP/y}$ GATA1-Cre platelets was tested in flow chamber experiments. Binding to a collagen-coated surface was measured in whole blood after labeling of platelets and normalization of platelet counts. Perfusion was performed under arterial shear condition (shear rate 1,500/s), which mediates binding of plasma VWF to surface-bound collagen (Ruggeri and Mendolicchio, 2007; Diener et al., 2009). Fluorescent FlnA-null platelets covered ~70% less of the collagen-coated surface than did WT platelets (Fig. 4, A and B). Considering that FlnA-null platelets are larger in size than WT platelets, this reveals a highly significant defect in binding to collagen-coated surface under arterial shear.

To test the hypothesis that the GPIbα defect might result from a decreased stability of ligand binding rather than a decreased initial binding efficiency, we analyzed individual platelet binding to the coated surface with high temporal resolution under the same experimental conditions (Fig. 4 C). After initial tethering, FlnA-null platelets showed significantly less firm adhesion than WT platelets. Although all WT platelets dwelled for at least 500 ms on the surface and 62% adhered firmly during the observation period, 23% of the FlnA-null platelets detached after <500 ms.

ITAM and ITAM-like signaling defects in FlnA-null platelets

The significance of FlnA expression in platelet responses to soluble agonists was tested (Fig. 5). Platelets isolated from FlnA$^{+/y}$ GATA1-Cre or FlnA$^{loxP/y}$ GATA1-Cre males were treated with GPCR agonists (i.e., ADP, the thromboxane analogue U46619, and/or epinephrine) and analyzed by flow cytometry using the antibody JON/A, which is specific for active αIIbβ3 (Fig. 5 A). ADP induced comparable αIIbβ3 activation in WT and FlnA-null platelets alone or in combination with U46619, epinephrine, or both. Furthermore, U46619 induced similar actin assembly responses in WT and FlnA-null platelets (unpublished data).

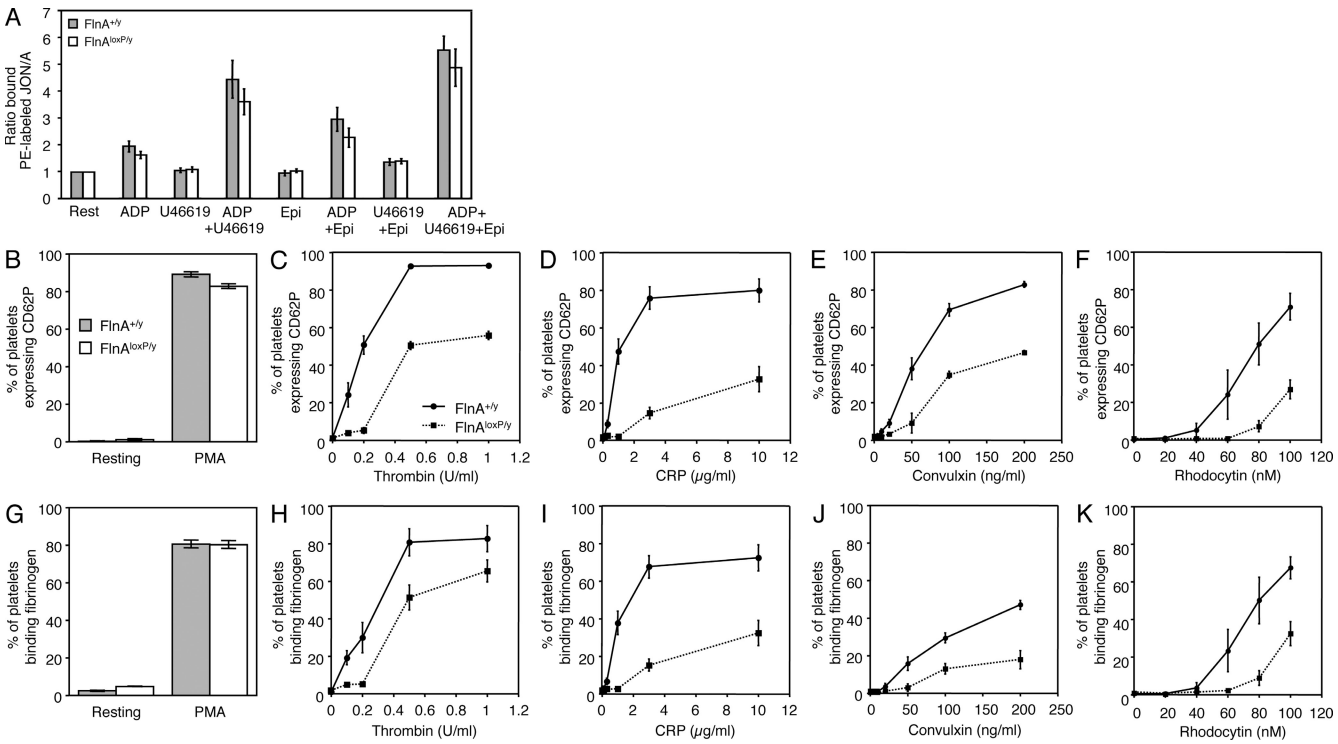

Figure 5. Functional defects in FlnA-null platelets. (A) FlnA$^{+/y}$ GATA1-Cre and FlnA$^{loxP/y}$ GATA1-Cre platelets in platelet-rich plasma (PRP) were activated with 10 μM ADP, 10 μM U46619, and/or 10 μM epinephrine (Epi), as indicated, and directly stained with PE-labeled JON/A for 10 min at room temperature. Platelets were then analyzed by flow cytometry. Results are the ratio between the mean fluorescence of activated versus resting platelets and represent the mean ± SD of four independent experiments. FlnA$^{+/y}$ GATA1-Cre and FlnA$^{loxP/y}$ GATA1-Cre platelets were activated with 50 nM PMA (B and G) or various concentrations of thrombin (C and H), CRP (D and I), convulxin (E and J), or rhodocytin (F and K) for 2 min at 37°C, as indicated. Platelets were then incubated with an FITC-labeled anti-mouse P-selectin antibody (B–F) or with Oregon green 488–labeled fibrinogen (G–K) and analyzed by flow cytometry. Results are expressed as percentage of positive platelets and represent mean ± SE of four independent experiments.

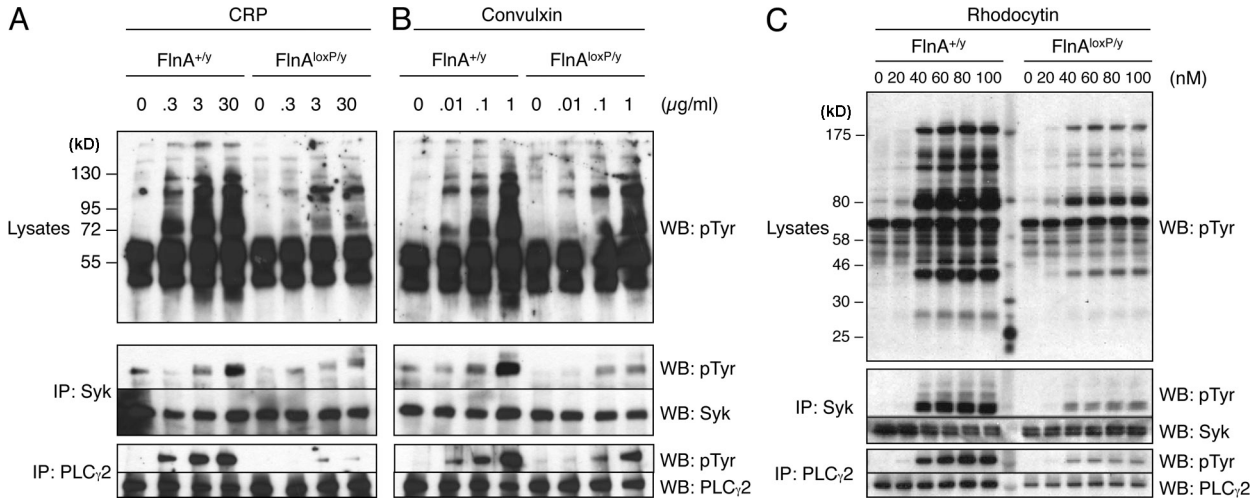

Figure 6. Protein tyrosine phosphorylation in platelets. FlnA$^{+/y}$ GATA1-Cre and FlnA$^{loxP/y}$ GATA1-Cre platelets were activated with CRP (A), convulxin (B), or rhodocytin (C) for 2 min at 37°C as indicated. Platelet lysates and Syk and PLC-γ2 were subjected to SDS-PAGE and probed with anti-Syk, anti-PLC-γ2, and anti-phosphotyrosine antibodies as indicated. Results are representative of three independent experiments.

The secretory and aggregatory capacities of FlnA-null platelets were further tested. WT and FlnA-null platelets were treated with PMA, which activates protein kinase C directly, and analyzed by flow cytometry for P-selectin (CD62P) expression, as a marker for α-granule secretion, or fibrinogen binding, as a marker for integrin αIIbβ3 activation (Falet et al., 2009). FlnA-null platelets expressed P-selectin and bound fibrinogen normally in response to PMA (Fig. 5, B and G).

Platelets isolated from FlnA$^{+/y}$ GATA1-Cre or FlnA$^{loxP/y}$ GATA1-Cre males were also treated with the GPCR agonist thrombin. Thrombin induced a concentration-dependent increase of P-selectin expression and fibrinogen binding in FlnA$^{+/y}$ GATA1-Cre platelets, reaching 93.1 ± 0.5% of P-selectin–expressing and 82.8 ± 6.9% of fibrinogen-binding platelets with 0.5 U/ml thrombin (Fig. 5, C and H). FlnA deficiency resulted in a significant decrease of platelet responses to thrombin, as only 55.9 ± 2.2% of P-selectin–expressing and 65.6 ± 5.9% of fibrinogen-binding platelets were obtained with 0.5 U/ml of thrombin.

Responses to CRP and convulxin, which are both specific for the collagen receptor GPVI (Watson et al., 2005), were severely affected by FlnA deficiency (Fig. 5, D, E, I, and J). Only 32.7 ± 6.7% of CD62P-expressing and 32.5 ± 6.6% of fibrinogen-binding FlnA$^{loxP/y}$ GATA1-Cre platelets were obtained with 10 μg/ml CRP, compared with 80.0 ± 6.2 and 72.5 ± 6.9% of FlnA$^{+/y}$ GATA1-Cre platelets, respectively. Similarly, only 42.6 ± 1.1% of P-selectin–expressing and 18.0 ± 4.8% of fibrinogen-binding FlnA$^{loxP/y}$ GATA1-Cre platelets were obtained with 200 ng/ml convulxin, compared with 82.8 ± 1.5% of P-selectin–expressing and 47.2 ± 2.3% of fibrinogen-binding FlnA$^{+/y}$ GATA1-Cre platelets, respectively.

To determine if the poor response to GPVI is extended to ITAM-like signaling, we assessed the ability of rhodocytin to activate WT and FlnA-null platelets through CLEC-2 (Suzuki-Inoue et al., 2006; Fig. 5, F and K). The data reveal that signals coming from CLEC-2 that lead to P-selectin expression and integrin αIIbβ3 activation were also highly diminished in FlnA-null platelets, in a similar fashion to those coming from GPVI.

Impaired tyrosine phosphorylation in FlnA-null platelets

The data described in the previous section suggest that FlnA modulates platelet signaling downstream of ITAM- and ITAM-like–containing receptors (i.e., GPVI and CLEC-2), cascades initiated by tyrosine phosphorylation, and activation of signaling proteins that include the protein tyrosine kinase Syk and phospholipase C-γ2 (PLC-γ2; Watson et al., 2005; Suzuki-Inoue et al., 2006). Hence, the ability of FlnA-null platelets to phosphorylate proteins on tyrosine in response to CRP, convulxin, or rhodocytin was investigated (Fig. 6). In FlnA$^{+/y}$ GATA1-Cre platelets, CRP, convulxin, and rhodocytin induced tyrosine phosphorylation of numerous platelet proteins, including a 130-kD protein that comigrates with PLC-γ2. The profile of tyrosine phosphorylation was markedly reduced in FlnA$^{loxP/y}$ GATA1-Cre platelets stimulated in the same conditions. Immunoprecipitation confirmed that Syk and PLC-γ2 phosphorylation was severely compromised in these platelets, thus revealing an important early role for FlnA in the ITAM- and ITAM-like–mediated signaling cascades (Fig. 6).

FlnA associates with Syk

Because the block in ITAM-based signaling in platelets occurs early, as judged by the decreased phosphorylation of Syk and PLC-γ2, we investigated whether FlnA interacts with any signaling molecules involved in the GPVI and CLEC-2 signaling pathways and found that FlnA directly binds to Syk. Syk immunoprecipitates were prepared from human platelet lysates and were probed against FlnA (Fig. 7 A). FlnA associated with immunoprecipitated Syk in both resting and CRP-activated platelets.

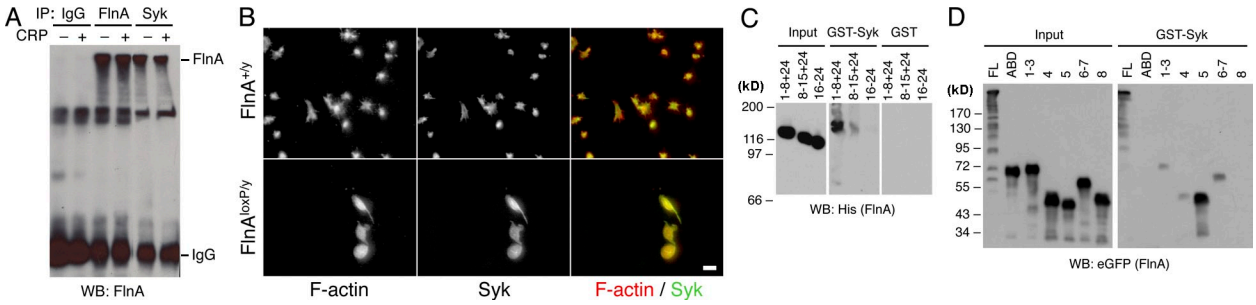

Figure 7. Syk associates with FlnA Ig repeat 5. (A) FlnA and Syk associate in platelets. Human platelets were activated, or not, with 3 µg/ml CRP for 2 min at 37°C. Syk and FlnA were immunoprecipitated with rabbit antibodies N19 and 4762, respectively. Immunoprecipitates were subjected to SDS-PAGE and probed for FlnA. A control rabbit IgG was used as negative control for specificity. Results are representative of two experiments. (B) FlnA restricts Syk to the periphery of spread platelets. $FlnA^{+/y}$ GATA1-Cre and $FlnA^{loxP/y}$ GATA1-Cre platelets were attached by centrifugation at 280 *g* for 5 min on CRP-coated coverslips, incubated by 5 min at 37°C, fixed with 3.7% formaldehyde for 20 min, permeabilized with 0.1% Triton in 1% BSA/PBS, and incubated with anti-Syk antibody BR15 followed by a secondary Alexa Fluor 488–conjugated anti-rabbit Ig antibody in PBS/1% BSA containing 0.1 µM rhodamine-phalloidin. Bar, 5 µm. Results are representative of two experiments. (C) 100 nM His-tagged FlnA recombinant truncates containing Ig repeats 1–8+24, 8–16+24, or 17–24 were incubated with 25 nM GST-Syk or GST alone as control. Complexes were pulled down with glutathione Sepharose beads, subjected to SDS-PAGE, and probed for His (FlnA) as indicated. Results are representative of four experiments. (D) 50 nM eGFP-tagged FlnA repeat fragments containing full-length FlnA (FL), its actin-binding domain (ABD), or Ig repeats 1–3, 4, 5, 6–7, or 8 were incubated with 500 nM GST-Syk. Complexes were pulled down with glutathione Sepharose beads, subjected to SDS-PAGE, and probed for eGFP (FlnA). Results are representative of four experiments.

The localization of Syk in WT and FlnA-null platelets was analyzed after adherence to CRP-coated surfaces. Fig. 7 B shows WT and FlnA-null platelets on CRP-coated surfaces after staining with rabbit anti-Syk antibody BR15 and Alexa Fluor 488–conjugated phalloidin and TRITC-labeled goat anti–rabbit IgG. Syk appears to be associated with the membrane in WT platelets and more cytoplasmic in FlnA-null platelets, indicating that FlnA contributes to Syk spatial distribution to the cytoplasmic surface of the platelet plasma membrane.

The FlnA–Syk interaction was further investigated in vitro using recombinant proteins. His-tagged FlnA constructs containing repeats 1–8+24, 8–15+24, or 16–24 were incubated with a fusion protein containing GST-Syk. The construct containing FlnA repeats 1–8+24 was pulled down by GST-Syk, but not GST alone, as indicated by anti-His immunoblotting (Fig. 7 C). Binding to repeats 8–15+24 and 16–24 was not detected, indicating that Syk binds to the FlnA N-terminal region containing repeats 1–8. We further determined that Syk binding occurs to FlnA repeat 5 (Fig. 7 D), as GST-His-Syk predominantly pulled down eGFP-tagged FlnA repeat 5. Weak binding to repeats 1–3, 4, and 6–7, but not to FlnA actin-binding domain and repeat 8, was also observed.

DISCUSSION

Our results show that $FlnA^{loxP/y}$ GATA1-Cre males have <15% of normal blood platelet count and increased tail bleeding time. These mice have enlarged platelets that lack FlnA. FlnA-null platelets lack normal actin membrane attachments and have decreased and altered GPIbα expression on their surface and impaired adhesion to collagen under flow conditions. Unexpectedly, FlnA-null platelets also have severe functional and signaling impairment in response to stimulation through ITAM- and ITAM-like–mediated signal receptors GPVI and CLEC-2, signaling which requires activation of the protein tyrosine kinase Syk. Interaction between platelet FlnA and Syk was detected by immunoprecipitation and reconstituted using purified proteins.

Because FlnA deficiency is embryonic lethal in mice (Feng et al., 2006; Hart et al., 2006), mice lacking FlnA in platelets were generated using the Cre–loxP system. $FlnA^{loxP/loxP}$ female mice were bred with erythroid/megakaryocytic-specific GATA1-Cre transgenic male mice. In agreement with the inactivation of the *PIGA* gene (Jasinski et al., 2001), we found that GATA1-Cre caused high efficiency *FLNA* gene inactivation in mouse megakaryocytes, as FlnA expression was absent in most platelets isolated from $FlnA^{loxP/y}$ GATA1-Cre male mice. A small population (<5%) of FlnA-containing platelets could be detected in some animals, suggesting mosaic GATA1-Cre expression, rendering incomplete $FlnA^{loxP}$ excision. Whether these platelets contain full-length FlnA or a truncated form, as shown for talin (Priddle et al., 1998), remains to be investigated. The high efficiency of gene inactivation is similar to that described for the widely used megakaryocyte-specific Pf4-Cre transgenic mouse and posits the GATA1-Cre mouse as a strong alternative for studies in megakaryocytes and platelets (Léon et al., 2007; Petrich et al., 2007; Tiedt et al., 2007; Hitchcock et al., 2008; Wen et al., 2009).

FlnA deficiency in $FlnA^{loxP}$ GATA1-Cre mice was associated with a high embryonic mortality, as our breeding strategy resulted in only 14.2% of pups being hemizygous FlnA-deficient males, which was lower than the expected 50%. GATA1-Cre is turned on early in embryogenesis and is also expressed outside of the hematopoietic system (Mao et al., 1999; Jasinski et al., 2001). Analysis of embryos collected at different stages of development showed complex developmental abnormalities, which is consistent with leaky Cre expression in early embryogenesis leading to $FlnA^{loxP}$ gene recombination in multiple nonhematopoietic tissues. The $FlnA^{loxP/y}$ GATA1-Cre

males that survived had a macrothrombocytopenia, with <15% of normal blood platelet count and ~2.5-fold enlarged platelets, but displayed no gross anatomical anomalies.

FlnA-null platelets had deleterious cytoskeletal alterations, resulting in inadequately cross-linked cytoplasmic actin filaments and poor attachment of the filaments to the membrane. FlnB expression levels appeared to be increased in FlnA-null platelets, compared with WT, which is consistent with a recently described compensatory FlnB expression increase in FlnA knockdown endothelial cells (Del Valle-Pérez et al., 2010). FlnB concentration levels, however, may be comparable in WT and FlnA-null platelets, relative to the increased volume and total protein content of FlnA-null platelets, compared with WT controls. Nevertheless, although FlnB has the same binding site for the cytoplasmic tail of GPIbα on repeat 17 (Nakamura et al., 2006), it does not compensate for FlnA absence, and no GPIbα was detected linked to F-actin in FlnA-null platelets. The F-actin/G-actin ratio at rest and the actin assembly reaction of FlnA-null platelets in response to thrombin were normal, as assessed by centrifugation of Triton X-100 platelet lysates and/or intracellular flow cytometry. The data show that the F-actin disassembly/assembly steps in the activation reaction occur normally in FlnA-null platelets, as described for FlnA-null fibroblasts (Feng et al., 2006; Hart et al., 2006).

As predicted, biochemical experiments revealed that all of the VWF receptor GPIbα was Triton X-100 soluble and, therefore, untethered to the actin cytoskeleton in FlnA-null platelets, resulting in a disorganized GPIbα topology on the platelet surface. Together, the data show that FlnA is required for normal platelet morphology and circulation and confirm that the macrothrombocytopenia associated with Bernard-Soulier syndrome results from the lack of the FlnA-GPIbα linkage to the actin cytoskeleton (Ware et al., 2000; Kanaji et al., 2002). Low platelet counts and large platelets have been described in periventricular heterotopia female patients (Parrini et al., 2006). These patients were carriers with only one mutant allele and are expected to have two platelet populations: one that is normal and one expressing mutant FlnA. $FlnA^{+/-}$ female mice have a mild thrombocytopenia with only 5% of their circulating platelets being FlnA null and enlarged. Further studies are required to determine the distribution of circulating FlnA-deficient platelets in periventricular heterotopia patients.

$FlnA^{loxP/y}$ GATA1-Cre males had a more severe bleeding phenotype than their macrothrombocytopenia would predict, indicating that FlnA-null platelets have functional defects. Indeed, there was loss of GPVI and GPIbα function in the absence of FlnA, as adhesion to collagen and collagen-associated VWF was diminished in FlnA-null platelets under flow conditions. Whether FlnA influences the ligand binding properties of GPIbα has been controversial in the literature. Some groups have reported that it enhances (Dong et al., 1997; Cranmer et al., 1999, 2005; Mistry et al., 2000; Williamson et al., 2002; Schade et al., 2003) and others that it diminishes (Englund et al., 2001). Our studies directly confirm the former, pointing out the importance of this interaction to platelet tethering under arterial shear conditions. Diminished binding to collagen and collagen-associated VWF and poor adherence under flow could result from the decreased density of GPIbα on the surface of FlnA-null platelets or from its changed topology.

Unexpectedly, FlnA-deficient platelets failed to respond normally to agonists for the ITAM- and ITAM-like–containing receptors GPVI or CLEC-2. In particular, the actin assembly reaction was blunted in response to rhodocytin (unpublished data) or CRP, but not thrombin. FlnA-null platelets also had decreased α-granule secretion and integrin αIIbβ3 activation. This diminished response is not a result of the lack of GPVI or CLEC-2, as FlnA-null platelets express normal or higher numbers of these receptors per cell (unpublished data). The possibility that FlnA-null platelets have general secretory and aggregatory defects was also eliminated because of their normal response to PMA, a direct activator of protein kinase C which bypasses ligation of platelet membrane receptors. Furthermore, αIIbβ3 activation in response to the GPCR agonist ADP alone or in combination with the thromboxane analogue U46619 and/or epinephrine was comparable between FlnA-null and WT platelets.

Platelets express at least three ITAM or ITAM-like–containing receptors: the low affinity IgG Fc receptor FcγRIIA, the collagen receptor GPVI–FcRγ chain complex, and CLEC-2. FcγRIIA is expressed on human but not mouse platelets. After ligation of GPVI with collagen, CRP, or convulxin, the two YXXL motifs of the associated FcRγ chain ITAM become phosphorylated by Src family kinases, i.e., Fyn and Lyn (Ezumi et al., 1998). Syk recognizes and binds the phosphorylated ITAM, leading to Syk autophosphorylation and activation (Poole et al., 1997). Downstream signals through adapter proteins, such as LAT and SLP-76, lead to PLC-γ2 phosphorylation and activation (Watson et al., 2005). Active PLC-γ2 hydrolyzes membrane bound polyphosphoinositides, notably phosphatidylinositol 4,5-bisphosphate, to form soluble inositol 1,4,5-trisphosphate, which releases cytosolic calcium from the internal stores, and membrane-bound 1,2-diacylglycerol, which activates protein kinase C. Signals are also sent to phosphoinositide 3-kinase, generating D3-containing polyphosphoinositides (Pasquet et al., 1999). CLEC-2 only contains a single YXXL motif but appears to be active as a dimer (Watson et al., 2009; Hughes et al., 2010) and signals through many of the same components as GPVI because platelets lacking LAT, SLP-76, or PLC-γ2 are not receptive to ligation of this receptor with rhodocytin (Suzuki-Inoue et al., 2006; Fuller et al., 2007).

We traced the failure of FlnA-null platelets to respond normally to agonists for GPVI or CLEC-2 to decreased Syk phosphorylation, which then poorly activates downstream signaling effectors such as PLC-γ2. Furthermore, Syk appeared to be cytoplasmic in FlnA-null platelets stimulated through GPVI rather than membrane associated as in WT controls. Together, the data indicate that FlnA contributes to Syk spatial distribution to the cytoplasmic surface of the platelet plasma membrane, a prerequisite for the docking to the ITAM or ITAM-like

sequences of GPVI and CLEC-2 and phosphorylation of Syk. This is a surprising finding and one that posits FlnA as essential for the very early Syk dependent steps in ITAM and ITAM-like based signaling.

Previous observations have suggested that GPVI and CLEC-2 must be coupled to the platelet cytoskeleton to function. CLEC-2 signaling is inhibited by cytochalasin D (Pollitt et al., 2010) and signaling of GPVI is greatly diminished by treating platelets with latrunculin A (unpublished data), an agent which depolymerizes actin filaments. The actin filament cross-linking activity of FlnA may be important for Syk recruitment and activation by the two receptors. FlnA and Syk were associated in both resting and activated platelets. Direct binding was reconstituted using purified Syk and FlnA fusion proteins and was restricted to Ig repeat 5 of FlnA using a series of FlnA truncates. Binding to FlnA Ig repeat 5 is novel, as most FlnA interacting partners bind to the C-terminal region containing Ig repeats 16–24 (Stossel et al., 2001; Feng and Walsh, 2004; Zhou et al., 2010). Mutations in FlnA Ig repeat 5 have been associated with familial cardiac valvular dystrophy (Kyndt et al., 2007). However, the consequence of these mutations on platelet activation remains to be determined, as does the location of the binding interface on Syk.

Stable platelet adhesion and aggregate formation under arterial shear condition, events which normally require activation of the αIIbβ3 integrin downstream of GPVI ligation by collagen and that of GPIbα by VWF, were severely impaired in the absence of FlnA (Ruggeri and Mendolicchio, 2007; Diener et al., 2009). Syk participates in the signaling cascade induced by GPIbα ligation, particularly in the calcium rise and activation of PI-3 kinase which follow ligation, and is intimately involved in downstream signaling to αIIbβ3 (Asazuma et al., 1997; Yanabu et al., 1997; Falati et al., 1999; Ozaki et al., 2005). It is likely that FlnA modulates Syk phosphorylation and activation downstream of GPIbα ligation as well. Further experimental evidence is required to test this hypothesis.

Our data further show that P-selectin expression and fibrinogen binding, but not actin assembly, were attenuated in FlnA-null platelets stimulated with the GPCR agonist thrombin. This could be a result of the altered expression and location of GPIbα, such that it is less able to present thrombin to its GPCR PAR4. Another explanation is that signals originated from GPVI or αIIbβ3 contribute to the thrombin signaling cascade. Boylan et al. (2006) have reported that platelets that lost GPVI after in vivo injection of an anti-GPVI antibody had diminished functional responses to thrombin and that outside-in signaling downstream of αIIbβ3 engagement also uses an ITAM-based pathway (Boylan et al., 2008). Older studies have shown that Syk is phosphorylated and activated after platelet stimulation with thrombin (Taniguchi et al., 1993; Clark et al., 1994). Thus, it is also possible that FlnA plays a yet undefined scaffolding role in thrombin receptor signaling.

In conclusion, our results show that FlnA is not only required for platelet morphology and circulation but also for signaling through platelet ITAM and ITAM-like containing receptors (i.e., GPVI and CLEC-2), which requires activation of the protein tyrosine kinase Syk. FlnA interacts with Syk through its Ig repeat 5 and, thus, docks Syk near the plasma membrane where it can bind GPVI, CLEC-2, and possibly GPIbα, initiating or reinforcing/amplifying their signaling cascades.

MATERIALS AND METHODS

Mice. $FlnA^{+/-}$ and $FlnA^{loxP/loxP}$ mice on a 129/Sv × C57BL/6 background were provided by Y. Feng and C. Walsh (Howard Hughes Medical Institute, Boston, MA; Feng et al., 2006). GATA1-Cre transgenic mice on a BALB/c background were provided by Y. Fujiwara and S.H. Orkin (Dana Farber Cancer Institute, Howard Hughes Medical Institute, Boston, MA; Jasinski et al., 2001). $FlnA^{loxP/loxP}$ females were bred with homozygous GATA1-Cre transgenic males to excise the floxed *FLNA* allele in the erythroid/megakaryocytic lineage. Mice were treated as approved by the Children's Hospital Animal Care and Use Committee.

Antibodies and reagents. Rabbit antibody directed against aa 1758–1767 of mouse FlnA (APQYNYPQGS) was produced by Invitrogen. Rabbit anti-FlnA antibody 4762 was purchased from Cell Signaling Technology. Rabbit anti-FlnB antibody and mouse anti-phosphotyrosine antibody 4G10 were purchased from Millipore. Mouse anti-phosphotyrosine antibody PY20 was obtained from BD. Rabbit anti-Syk antibody BR15 was supplied by M. Tomlinson (DNAX Research Institute, Palo Alto, CA). Control rabbit antibody, rabbit anti-Syk antibody N19, and rabbit anti–PLC-γ2 Q20 were obtained from Santa Cruz Biotechnology, Inc. Antibodies directed against mouse GPIbα (CD42b), GPIbβ (CD42c), GPIX (CD42a), GPV (CD42d), GPVI, and active αIIbβ3 were obtained from Emfret Analytics. Antibodies directed against mouse P-selectin (CD62P) and GPIIIa (CD61 and integrin β3) were obtained from BD. CM-Orange, Oregon green 488–labeled fibrinogen, and Alexa Fluor 488–labeled donkey anti–mouse IgG and anti–rabbit IgG antibodies were obtained from Invitrogen. Protein G Sepharose and glutathione Sepharose beads were obtained from GE Healthcare. The CRP (amino acids $GCO(GPP)_{10}GCOG$) was synthesized by the Tufts University Core Facility and cross-linked as described previously (Morton et al., 1995). Rhodocytin was purified from the venom of *Callose-lasma rhodostoma* (Suzuki-Inoue et al., 2006). ADP was obtained from Chrono-log and U46619 from Enzo Life Sciences. All other reagents were of the highest purity available (Sigma-Aldrich).

Complete blood count. Blood was collected from mice by retroorbital plexus bleeding in EDTA. Peripheral blood platelet count was performed using an ADVIA 120/2120 automated hematology analyzer (Bayer HealthCare; Falet et al., 2009).

Bleeding time assay. Mouse tail bleeding times were determined by snipping 5 mm of distal mouse tail and immediately immersing the tail in 37°C isotonic saline (Ware et al., 2000). A complete cessation of bleeding was defined as the bleeding time. Measurements exceeding 10 min were stopped by cauterization of the tail. Data were statistically analyzed by the Kaplan-Meier method (Kaplan and Meier, 1958).

Platelet preparation. Blood was collected from mice by retroorbital plexus bleeding and anticoagulated in ACD for experiments with washed platelets or in citrate for experiments with PRP. Mouse PRP was obtained by centrifugation of the blood at 100 *g* for 8 min, followed by centrifugation of the supernatant and the buffy coat at 100 *g* for 6 min. Mouse platelets were isolated by two sequential centrifugations of the PRP at 1,200 *g* for 5 min in 140 mM NaCl, 5 mM KCl, 12 mM trisodium citrate, 10 mM glucose, and 12.5 mM sucrose, pH 6.0 (washing buffer), and resuspended in 10 mM Hepes, 140 mM NaCl, 3 mM KCl, 0.5 mM $MgCl_2$, 5 mM $NaHCO_3$, and 10 mM glucose, pH 7.4 (resuspension buffer), as previously described (Hoffmeister et al., 2003). Platelet concentration was adjusted to $2–5 \times 10^8$/ml depending on the assay performed, and platelets were allowed to rest for 30 min before use.

Flow cytometry. Washed platelets were fixed and permeabilized in Cytofix/Cytoperm solution (BD), washed in Perm/Wash solution (BD), and incubated with a rabbit anti-FlnA antibody or a rabbit anti-FlnB antibody, followed by Alexa Fluor 488–labeled donkey anti–rabbit IgG antibody. For the actin assembly assay, resting or activated, fixed, and permeabilized platelets were incubated with 2 μM TRITC-labeled phalloidin (Falet et al., 2009).

For the functional assays, resting or activated washed platelets were incubated with a FITC-labeled anti–P-selectin antibody or Oregon green 488–labeled fibrinogen for 30 min at room temperature (Falet et al., 2009). Platelets were activated in PRP in the presence of PE-labeled JON/A. Fluorescence was quantified using a FACSCalibur flow cytometer (BD). A total of 20,000 events were analyzed for each sample.

Platelet cytoskeletal rearrangements. Platelets were activated by attachment to CRP-coated coverslips for 10 min at 37°C. For F-actin staining in the light microscope, they were incubated with 0.1 μM Alexa Fluor 568–conjugated phalloidin after fixation with 1% formaldehyde, permeabilization with 0.1% Triton X-100, and appropriate washing and blocking. For electron microscopy, the CRP-attached and activated platelets were permeabilized with 0.75% Triton in PHEM buffer for 2 min at 37°C, washed in PHEM without Triton X-100, and then fixed with 1% glutaraldehyde in PHEM for 10 min. The samples were washed into water and rapidly frozen by slamming them into a liquid helium–cooled copper block. Frozen samples were transferred to a liquid nitrogen–cooled stage on a CFE-60 apparatus (Cressington), warmed to −80°C for 60 min, and metal cast with 1.4 nm tantalum-tungsten at 45° with rotation and 5 nm of carbon at 90° without rotation. Metal replicas were floated from the coverslips in 25% hydrofluoric acid, water washed, and examined by transmission electron microscopy (JEOL 1200 EX).

Immunogold anti-GPIbα glycoprotein labeling. Resting platelets were attached to polylysine-coated coverslips by centrifugation at 300 *g* for 5 min in PBS containing 0.1% glutaraldehyde. They were fixed for 5 min in 0.5% glutaraldehyde in PBS, unreacted aldehydes blocked using a 2 min incubation with 0.1% sodium borohydride, and washed into PBS/BSA. The platelets were surface labeled with a rat anti-GPIbα monoclonal antibody. After washing, platelets were incubated with 10 nm of gold coated with goat anti–rat IgG. They were washed, postfixed with 1% gluteraldehyde for 10 min, washed into water, and processed by rapid freezing, freeze drying, and metal casting.

SDS-PAGE and immunoblot analysis. Platelets were lysed at 4°C in 1% Nonidet P-40, 150 mM NaCl, and 50 mM Tris, pH 7.4, containing 1 mM EGTA, 1 mM Na_3VO_4, and Complete protease inhibitor cocktail (Roche). SDS-PAGE sample buffer containing 5% β-mercaptoethanol was added. After boiling for 5 min, platelet proteins were separated on 8% polyacrylamide gels and transferred onto an Immobilon-P membrane (Millipore). Membranes were incubated overnight in 0.2% Tween-20, 100 mM NaCl, and 20 mM Tris, pH 7.4, containing 1% BSA, and then probed with antibodies directed against proteins of interest. Detection was performed with an enhanced chemiluminescence system (Thermo Fisher Scientific).

For the immunoprecipitation studies, Nonidet P-40 lysates were centrifuged at 14,000 *g* for 10 min at 4°C. Soluble fractions were incubated with antibodies directed against proteins of interest for 2 h at 4°C, followed by incubation with protein G–conjugated Sepharose beads for 1 h at 4°C. After washing, immune complexes were resolved by SDS-PAGE as described in this section.

For the purified recombinant protein binding assays, His-tagged and eGFP-tagged FlnA fragments were expressed in Sf9 cells and purified as described previously (Nakamura et al., 2007). GST-Syk was purchased from Active Motif. FlnA fragments and GST-Syk were incubated for 2 h at room temperature in 1% Nonidet P-40, 150 mM NaCl, and 50 mM Tris, pH 7.4, containing 1 mM EGTA, 1 mM Na_3VO_4, and Complete protease inhibitor cocktail, followed by incubation with glutathione conjugated Sepharose beads for 1 h. After washing, immune complexes were resolved by SDS-PAGE as described in this section.

Flow chamber studies. Blood was collected from mice by retroorbital plexus bleeding and anticoagulated in 40 μM PPACK and 20 μg/ml enoxaparin. PRP was separated by centrifugation at 80 *g* for 6 min and purified at 180 *g* for 5 min for WT and at 80 *g* for 5 min for FlnA-null platelets, respectively. Platelets were collected by centrifugation at 640 *g* for 6 min in the presence of 2 μg/ml prostacyclin and resuspended in modified Tyrode's buffer (140 mM NaCl, 0.36 mM Na_2HPO_4, 3 mM KCl, 12 mM $NaHCO_3$, 5 mM Hepes, and 10 mM glucose, pH 7.3) containing 0.2% BSA and labeled with 2.5 mg/ml calcein orange. Platelet-poor blood was reconstituted with labeled platelets and remaining plasma at 10^8/ml platelets. Using a 0.0127-cm silicon rubber gasket, a parallel plate flow chamber (GlycoTech) was assembled onto 35-mm diameter round glass coverslips, which had been coated with 100 μg/ml collagen type I (Nycomed). Perfusion was performed at a shear rate of 1,500/s for 3 min. Platelet adhesion to collagen-associated plasma VWF was monitored with an Axiovert 135 inverted microscope (Carl Zeiss, Inc.) at 32× and a silicon-intensified tube camera C 2400 (Hamamatsu Photonics) and analyzed with Image SXM 1.62 (National Institutes of Health).

Statistical analysis. Statistical analysis was performed using the unpaired Student's *t* test. A p-value <0.05 was considered statistically significant.

We thank Drs. Yuanyi Feng and Christopher Walsh for providing the $FlnA^{+/-}$ and $FlnA^{loxP/loxP}$ mice, Drs. Yuko Fujiwara and Stuart Orkin for providing the GATA1-Cre mice, Dr. Mike Tomlinson for the anti-Syk antibody, and Teresa Collins and Dr. Fumihiko Nakamura for the recombinant FlnA constructs. We thank Drs. Karin Hoffmeister and Larry Frelinger for advice and reagents, Dr. François Maignen for statistical expertise, and Mike Marchetti for technical help.

This work was supported by National Institutes of Health grants HL-056252 (J.H. Hartwig), HL-056949 (J.H. Hartwig and D.D. Wagner), and HL-059561 (J.H. Hartwig and H. Falet). A.Y. Pollitt was supported by the British Heart Foundation (BHF) project grant (PG/07/116). S.P. Watson holds a BHF Chair.

The authors have no conflicting financial interests.

Submitted: 2 February 2010
Accepted: 23 July 2010

REFERENCES

Asazuma, N., Y. Ozaki, K. Satoh, Y. Yatomi, M. Handa, Y. Fujimura, S. Miura, and S. Kume. 1997. Glycoprotein Ib-von Willebrand factor interactions activate tyrosine kinases in human platelets. *Blood*. 90:4789–4798.

Boylan, B., M.C. Berndt, M.L. Kahn, and P.J. Newman. 2006. Activation-independent, antibody-mediated removal of GPVI from circulating human platelets: development of a novel NOD/SCID mouse model to evaluate the in vivo effectiveness of anti-human platelet agents. *Blood*. 108:908–914. doi:10.1182/blood-2005-07-2937

Boylan, B., C. Gao, V. Rathore, J.C. Gill, D.K. Newman, and P.J. Newman. 2008. Identification of FcgammaRIIa as the ITAM-bearing receptor mediating alphaIIbbeta3 outside-in integrin signaling in human platelets. *Blood*. 112:2780–2786. doi:10.1182/blood-2008-02-142125

Clark, E.A., S.J. Shattil, M.H. Ginsberg, J. Bolen, and J.S. Brugge. 1994. Regulation of the protein tyrosine kinase pp72syk by platelet agonists and the integrin α IIb beta 3. *J. Biol. Chem.* 269:28859–28864.

Cranmer, S.L., P. Ulsemer, B.M. Cooke, H.H. Salem, C. de la Salle, F. Lanza, and S.P. Jackson. 1999. Glycoprotein (GP) Ib-IX-transfected cells roll on a von Willebrand factor matrix under flow. Importance of the GPib/actin-binding protein (ABP-280) interaction in maintaining adhesion under high shear. *J. Biol. Chem.* 274:6097–6106. doi:10.1074/jbc.274.10.6097

Cranmer, S.L., I. Pikovski, P. Mangin, P.E. Thompson, T. Domagala, M. Frazzetto, H.H. Salem, and S.P. Jackson. 2005. Identification of a unique filamin A binding region within the cytoplasmic domain of glycoprotein Ibalpha. *Biochem. J.* 387:849–858. doi:10.1042/BJ20041836

Cunningham, C.C., J.B. Gorlin, D.J. Kwiatkowski, J.H. Hartwig, P.A. Janmey, H.R. Byers, and T.P. Stossel. 1992. Actin-binding protein

requirement for cortical stability and efficient locomotion. *Science*. 255:325–327. doi:10.1126/science.1549777

David, T., P. Ohlmann, A. Eckly, S. Moog, J.-P. Cazenave, C. Gachet, and F. Lanza. 2006. Inhibition of adhesive and signaling functions of the platelet GPIb-V-IX complex by a cell penetrating GPIbalpha peptide. *J. Thromb. Haemost.* 4:2645–2655. doi:10.1111/j.1538-7836.2006.02198.x

Del Valle-Pérez, B., V.G. Martínez, C. Lacasa-Salavert, A. Figueras, S.S. Shapiro, T. Takafuta, O. Casanovas, G. Capellà, F. Ventura, and F. Viñals. 2010. Filamin B plays a key role in vascular endothelial growth factor-induced endothelial cell motility through its interaction with Rac-1 and Vav-2. *J. Biol. Chem.* 285:10748–10760. doi:10.1074/jbc.M109.062984

Diener, J.L., H.A. Daniel Lagassé, D. Duerschmied, Y. Merhi, J.F. Tanguay, R. Hutabarat, J. Gilbert, D.D. Wagner, and R. Schaub. 2009. Inhibition of von Willebrand factor-mediated platelet activation and thrombosis by the anti-von Willebrand factor A1-domain aptamer ARC1779. *J. Thromb. Haemost.* 7:1155–1162. doi:10.1111/j.1538-7836.2009.03459.x

Dong, J.F., C.Q. Li, G. Sae-Tung, W. Hyun, V. Afshar-Kharghan, and J.A. López. 1997. The cytoplasmic domain of glycoprotein (GP) Ibalpha constrains the lateral diffusion of the GP Ib-IX complex and modulates von Willebrand factor binding. *Biochemistry*. 36:12421–12427. doi:10.1021/bi970636b

Englund, G.D., R.J. Bodnar, Z. Li, Z.M. Ruggeri, and X. Du. 2001. Regulation of von Willebrand factor binding to the platelet glycoprotein Ib-IX by a membrane skeleton-dependent inside-out signal. *J. Biol. Chem.* 276:16952–16959. doi:10.1074/jbc.M008048200

Ezumi, Y., K. Shindoh, M. Tsuji, and H. Takayama. 1998. Physical and functional association of the Src family kinases Fyn and Lyn with the collagen receptor glycoprotein VI-Fc receptor γ chain complex on human platelets. *J. Exp. Med.* 188:267–276. doi:10.1084/jem.188.2.267

Falati, S., C.E. Edmead, and A.W. Poole. 1999. Glycoprotein Ib-V-IX, a receptor for von Willebrand factor, couples physically and functionally to the Fc receptor γ-chain, Fyn, and Lyn to activate human platelets. *Blood*. 94:1648–1656.

Falet, H., K.M. Hoffmeister, R. Neujahr, J.E. Italiano Jr., T.P. Stossel, F.S. Southwick, and J.H. Hartwig. 2002. Importance of free actin filament barbed ends for Arp2/3 complex function in platelets and fibroblasts. *Proc. Natl. Acad. Sci. USA*. 99:16782–16787. doi:10.1073/pnas.222652499

Falet, H., M.P. Marchetti, K.M. Hoffmeister, M.J. Massaad, R.S. Geha, and J.H. Hartwig. 2009. Platelet-associated IgAs and impaired GPVI responses in platelets lacking WIP. *Blood*. 114:4729–4737. doi:10.1182/blood-2009-02-202721

Feng, Y., and C.A. Walsh. 2004. The many faces of filamin: a versatile molecular scaffold for cell motility and signalling. *Nat. Cell Biol.* 6:1034–1038. doi:10.1038/ncb1104-1034

Feng, S., J.C. Reséndiz, X. Lu, and M.H. Kroll. 2003. Filamin A binding to the cytoplasmic tail of glycoprotein Ibalpha regulates von Willebrand factor-induced platelet activation. *Blood*. 102:2122–2129. doi:10.1182/blood-2002-12-3805

Feng, S., X. Lu, and M.H. Kroll. 2005. Filamin A binding stabilizes nascent glycoprotein Ibalpha trafficking and thereby enhances its surface expression. *J. Biol. Chem.* 280:6709–6715. doi:10.1074/jbc.M413590200

Feng, Y., M.H. Chen, I.P. Moskowitz, A.M. Mendonza, L. Vidali, F. Nakamura, D.J. Kwiatkowski, C.A. Walsh, D.J. Kwiatkowski, and C.A. Walsh. 2006. Filamin A (FLNA) is required for cell-cell contact in vascular development and cardiac morphogenesis. *Proc. Natl. Acad. Sci. USA*. 103:19836–19841. doi:10.1073/pnas.0609628104

Flanagan, L.A., J. Chou, H. Falet, R. Neujahr, J.H. Hartwig, and T.P. Stossel. 2001. Filamin A, the Arp2/3 complex, and the morphology and function of cortical actin filaments in human melanoma cells. *J. Cell Biol.* 155:511–517. doi:10.1083/jcb.200105148

Fox, J.E.B. 1985a. Identification of actin-binding protein as the protein linking the membrane skeleton to glycoproteins on platelet plasma membranes. *J. Biol. Chem.* 260:11970–11977.

Fox, J.E.B. 1985b. Linkage of a membrane skeleton to integral membrane glycoproteins in human platelets. Identification of one of the glycoproteins as glycoprotein Ib. *J. Clin. Invest.* 76:1673–1683. doi:10.1172/JCI112153

Fox, J.W., E.D. Lamperti, Y.Z. Ekşioğlu, S.E. Hong, Y. Feng, D.A. Graham, I.E. Scheffer, W.B. Dobyns, B.A. Hirsch, R.A. Radtke, et al. 1998. Mutations in filamin 1 prevent migration of cerebral cortical neurons in human periventricular heterotopia. *Neuron*. 21:1315–1325. doi:10.1016/S0896-6273(00)80651-0

Fuller, G.L., J.A. Williams, M.G. Tomlinson, J.A. Eble, S.L. Hanna, S. Pöhlmann, K. Suzuki-Inoue, Y. Ozaki, S.P. Watson, and A.C. Pearce. 2007. The C-type lectin receptors CLEC-2 and Dectin-1, but not DC-SIGN, signal via a novel YXXL-dependent signaling cascade. *J. Biol. Chem.* 282:12397–12409. doi:10.1074/jbc.M609558200

Hart, A.W., J.E. Morgan, J. Schneider, K. West, L. McKie, S. Bhattacharya, I.J. Jackson, and S.H. Cross. 2006. Cardiac malformations and midline skeletal defects in mice lacking filamin A. *Hum. Mol. Genet.* 15:2457–2467. doi:10.1093/hmg/ddl168

Hitchcock, I.S., N.E. Fox, N. Prévost, K. Sear, S.J. Shattil, and K. Kaushansky. 2008. Roles of focal adhesion kinase (FAK) in megakaryopoiesis and platelet function: studies using a megakaryocyte lineage specific FAK knockout. *Blood*. 111:596–604. doi:10.1182/blood-2007-05-089680

Hoffmeister, K.M., T.W. Felbinger, H. Falet, C.V. Denis, W. Bergmeier, T.N. Mayadas, U.H. von Andrian, D.D. Wagner, T.P. Stossel, and J.H. Hartwig. 2003. The clearance mechanism of chilled blood platelets. *Cell*. 112:87–97. doi:10.1016/S0092-8674(02)01253-9

Hughes, C.E., A.Y. Pollitt, J. Mori, J.A. Eble, M.G. Tomlinson, J.H. Hartwig, C.A. O'Callaghan, K. Fütterer, and S.P. Watson. 2010. CLEC-2 activates Syk through dimerization. *Blood*. 115:2947–2955. doi:10.1182/blood-2009-08-237834

Jasinski, M., P. Keller, Y. Fujiwara, S.H. Orkin, and M. Bessler. 2001. GATA1-Cre mediates Piga gene inactivation in the erythroid/megakaryocytic lineage and leads to circulating red cells with a partial deficiency in glycosyl phosphatidylinositol-linked proteins (paroxysmal nocturnal hemoglobinuria type II cells). *Blood*. 98:2248–2255. doi:10.1182/blood.V98.7.2248

Kanaji, T., S. Russell, and J. Ware. 2002. Amelioration of the macrothrombocytopenia associated with the murine Bernard-Soulier syndrome. *Blood*. 100:2102–2107. doi:10.1182/blood-2002-03-0997

Kaplan, E.L., and P. Meier. 1958. Nonparametric estimation from incomplete observations. *J. Am. Stat. Assoc.* 53:457–481. doi:10.2307/2281868

Kyndt, F., J.P. Gueffet, V. Probst, P. Jaafar, A. Legendre, F. Le Bouffant, C. Toquet, E. Roy, L. McGregor, S.A. Lynch, et al. 2007. Mutations in the gene encoding filamin A as a cause for familial cardiac valvular dystrophy. *Circulation*. 115:40–49. doi:10.1161/CIRCULATIONAHA.106.622621

Léon, C., A. Eckly, B. Hechler, B. Aleil, M. Freund, C. Ravanat, M. Jourdain, C. Nonne, J. Weber, R. Tiedt, et al. 2007. Megakaryocyte-restricted MYH9 inactivation dramatically affects hemostasis while preserving platelet aggregation and secretion. *Blood*. 110:3183–3191. doi:10.1182/blood-2007-03-080184

Mao, X., Y. Fujiwara, and S.H. Orkin. 1999. Improved reporter strain for monitoring Cre recombinase-mediated DNA excisions in mice. *Proc. Natl. Acad. Sci. USA*. 96:5037–5042. doi:10.1073/pnas.96.9.5037

Mistry, N., S.L. Cranmer, Y. Yuan, P. Mangin, S.M. Dopheide, I. Harper, S. Giuliano, D.E. Dunstan, F. Lanza, H.H. Salem, and S.P. Jackson. 2000. Cytoskeletal regulation of the platelet glycoprotein Ib/V/IX-von willebrand factor interaction. *Blood*. 96:3480–3489.

Morton, L.F., P.G. Hargreaves, R.W. Farndale, R.D. Young, and M.J. Barnes. 1995. Integrin α 2 β 1-independent activation of platelets by simple collagen-like peptides: collagen tertiary (triple-helical) and quaternary (polymeric) structures are sufficient alone for α 2 β 1-independent platelet reactivity. *Biochem. J.* 306:337–344.

Nakamura, F., R. Pudas, O. Heikkinen, P. Permi, I. Kilpeläinen, A.D. Munday, J.H. Hartwig, T.P. Stossel, and J. Ylänne. 2006. The structure of the GPIb-filamin A complex. *Blood*. 107:1925–1932. doi:10.1182/blood-2005-10-3964

Nakamura, F., T.M. Osborn, C.A. Hartemink, J.H. Hartwig, and T.P. Stossel. 2007. Structural basis of filamin A functions. *J. Cell Biol.* 179:1011–1025. doi:10.1083/jcb.200707073

Ozaki, Y., N. Asazuma, K. Suzuki-Inoue, and M.C. Berndt. 2005. Platelet GPIb-IX-V-dependentsignaling.*J. Thromb. Haemost.*3:1745–1751.doi:10.1111/j.1538-7836.2005.01379.x

Parrini, E., A. Ramazzotti, W.B. Dobyns, D. Mei, F. Moro, P. Veggiotti, C. Marini, E.H. Brilstra, B. Dalla Bernardina, L. Goodwin, et al. 2006. Periventricular heterotopia: phenotypic heterogeneity and correlation with Filamin A mutations. *Brain*. 129:1892–1906. doi:10.1093/brain/awl125

Pasquet, J.-M., R. Bobe, B. Gross, M.P. Gratacap, M.G. Tomlinson, B. Payrastre, and S.P. Watson. 1999. A collagen-related peptide regulates phospholipase Cgamma2 via phosphatidylinositol 3-kinase in human platelets. *Biochem. J.* 342:171–177. doi:10.1042/0264-6021:3420171

Petrich, B.G., P. Marchese, Z.M. Ruggeri, S. Spiess, R.A. Weichert, F. Ye, R. Tiedt, R.C. Skoda, S.J. Monkley, D.R. Critchley, and M.H. Ginsberg. 2007. Talin is required for integrin-mediated platelet function in hemostasis and thrombosis. *J. Exp. Med.* 204:3103–3111. doi:10.1084/jem.20071800

Pollitt, A.Y., B. Grygielska, B. Leblond, L. Désiré, J.A. Eble, and S.P. Watson. 2010. Phosphorylation of CLEC-2 is dependent on lipid rafts, actin polymerization, secondary mediators, and Rac. *Blood*. 115:2938–2946. doi:10.1182/blood-2009-12-257212

Poole, A., J.M. Gibbins, M. Turner, M.J. van Vugt, J.G. van de Winkel, T. Saito, V.L. Tybulewicz, and S.P. Watson. 1997. The Fc receptor γ-chain and the tyrosine kinase Syk are essential for activation of mouse platelets by collagen. *EMBO J.* 16:2333–2341. doi:10.1093/emboj/16.9.2333

Priddle, H., L. Hemmings, S. Monkley, A. Woods, B. Patel, D. Sutton, G.A. Dunn, D. Zicha, and D.R. Critchley. 1998. Disruption of the talin gene compromises focal adhesion assembly in undifferentiated but not differentiated embryonic stem cells. *J. Cell Biol.* 142:1121–1133. doi:10.1083/jcb.142.4.1121

Pudas, R., T.R. Kiema, P.J. Butler, M. Stewart, and J. Ylänne. 2005. Structural basis for vertebrate filamin dimerization. *Structure*. 13:111–119. doi:10.1016/j.str.2004.10.014

Robertson, S.P. 2005. Filamin A: phenotypic diversity. *Curr. Opin. Genet. Dev.* 15:301–307. doi:10.1016/j.gde.2005.04.001

Robertson, S.P., S.R.F. Twigg, A.J. Sutherland-Smith, V. Biancalana, R.J. Gorlin, D. Horn, S.J. Kenwrick, C.A. Kim, E. Morava, R. Newbury-Ecob, et al; OPD-spectrum Disorders Clinical Collaborative Group. 2003. Localized mutations in the gene encoding the cytoskeletal protein filamin A cause diverse malformations in humans. *Nat. Genet.* 33:487–491. doi:10.1038/ng1119

Ruggeri, Z.M., and G.L. Mendolicchio. 2007. Adhesion mechanisms in platelet function. *Circ. Res.* 100:1673–1685. doi:10.1161/01.RES.0000267878.97021.ab

Schade, A.J., M. Arya, S. Gao, R. Diz-Küçükkaya, B. Anvari, L.V. McIntire, J.A. López, and J.F. Dong. 2003. Cytoplasmic truncation of glycoprotein Ib α weakens its interaction with von Willebrand factor and impairs cell adhesion. *Biochemistry*. 42:2245–2251. doi:10.1021/bi026549n

Sheen, V.L., A. Jansen, M.H. Chen, E. Parrini, T. Morgan, R. Ravenscroft, V. Ganesh, T. Underwood, J. Wiley, R. Leventer, et al. 2005. Filamin A mutations cause periventricular heterotopia with Ehlers-Danlos syndrome. *Neurology*. 64:254–262.

Stossel, T.P., J. Condeelis, L. Cooley, J.H. Hartwig, A. Noegel, M. Schleicher, and S.S. Shapiro. 2001. Filamins as integrators of cell mechanics and signalling. *Nat. Rev. Mol. Cell Biol.* 2:138–145. doi:10.1038/35052082

Suzuki-Inoue, K., G.L. Fuller, A. García, J.A. Eble, S. Pöhlmann, O. Inoue, T.K. Gartner, S.C. Hughan, A.C. Pearce, G.D. Laing, et al. 2006. A novel Syk-dependent mechanism of platelet activation by the C-type lectin receptor CLEC-2. *Blood*. 107:542–549. doi:10.1182/blood-2005-05-1994

Taniguchi, T., H. Kitagawa, S. Yasue, S. Yanagi, K. Sakai, M. Asahi, S. Ohta, F. Takeuchi, S. Nakamura, and H. Yamamura. 1993. Protein-tyrosine kinase p72syk is activated by thrombin and is negatively regulated through Ca^{2+} mobilization in platelets. *J. Biol. Chem.* 268:2277–2279.

Tiedt, R., T. Schomber, H. Hao-Shen, and R.C. Skoda. 2007. Pf4-Cre transgenic mice allow the generation of lineage-restricted gene knockouts for studying megakaryocyte and platelet function in vivo. *Blood*. 109:1503–1506. doi:10.1182/blood-2006-04-020362

Unger, S., A. Mainberger, C. Spitz, A. Bähr, C. Zeschnigk, B. Zabel, A. Superti-Furga, and D.J. Morris-Rosendahl. 2007. Filamin A mutation is one cause of FG syndrome. *Am. J. Med. Genet. A*. 143A:1876–1879. doi:10.1002/ajmg.a.31751

Ware, J., S. Russell, and Z.M. Ruggeri. 2000. Generation and rescue of a murine model of platelet dysfunction: the Bernard-Soulier syndrome. *Proc. Natl. Acad. Sci. USA*. 97:2803–2808. doi:10.1073/pnas.050582097

Watson, S.P., J.M. Auger, O.J. McCarty, and A.C. Pearce. 2005. GPVI and integrin alphaIIb beta3 signaling in platelets. *J. Thromb. Haemost.* 3:1752–1762. doi:10.1111/j.1538-7836.2005.01429.x

Watson, A.A., C.M. Christou, J.R. James, A.E. Fenton-May, G.E. Moncayo, A.R. Mistry, S.J. Davis, R.J. Gilbert, A. Chakera, and C.A. O'Callaghan. 2009. The platelet receptor CLEC-2 is active as a dimer. *Biochemistry*. 48:10988–10996. doi:10.1021/bi901427d

Wen, Q., C. Leung, Z. Huang, S. Small, A.L. Reddi, J.D. Licht, and J.D. Crispino. 2009. Survivin is not required for the endomitotic cell cycle of megakaryocytes. *Blood*. 114:153–156. doi:10.1182/blood-2008-11-190801

Williamson, D., I. Pikovski, S.L. Cranmer, P. Mangin, N. Mistry, T. Domagala, S. Chehab, F. Lanza, H.H. Salem, and S.P. Jackson. 2002. Interaction between platelet glycoprotein Ibalpha and filamin-1 is essential for glycoprotein Ib/IX receptor anchorage at high shear. *J. Biol. Chem.* 277:2151–2159. doi:10.1074/jbc.M109384200

Yanabu, M., Y. Ozaki, S. Nomura, T. Miyake, Y. Miyazaki, H. Kagawa, Y. Yamanaka, N. Asazuma, K. Satoh, S. Kume, et al. 1997. Tyrosine phosphorylation and p72syk activation by an anti-glycoprotein Ib monoclonal antibody. *Blood*. 89:1590–1598.

Zhou, A.X., J.H. Hartwig, and L.M. Akyürek. 2010. Filamins in cell signaling, transcription and organ development. *Trends Cell Biol.* 20:113–123. doi:10.1016/j.tcb.2009.12.001